SAND2014-16106C

Solar optical codes evaluation for modeling and analyzing complex solar receiver geometries

Julius Yellowhair*, Jesus D. Ortega, Joshua M. Christian, Clifford K. Ho
Sandia National Laboratories, Concentrating Solar Technologies
P.O. Box 5800, Albuquerque, NM, 87185 USA

ABSTRACT

Solar optical modeling tools are valuable for modeling and predicting the performance of solar technology systems. Four optical modeling tools were evaluated using the National Solar Thermal Test Facility heliostat field combined with flat plate receiver geometry as a benchmark. The four optical modeling tools evaluated were DELSOL, HELIOS, SolTrace, and Tonatiuh. All are available for free from their respective developers. DELSOL and HELIOS both use a convolution of the sunshape and optical errors for rapid calculation of the incident irradiance profiles on the receiver surfaces. SolTrace and Tonatiuh use ray-tracing methods to intersect the reflected solar rays with the receiver surfaces and construct irradiance profiles. We found the ray-tracing tools, although slower in computation speed, to be more flexible for modeling complex receiver geometries, whereas DELSOL and HELIOS were limited to standard receiver geometries such as flat plate, cylinder, and cavity receivers. We also list the strengths and deficiencies of the tools to show tool preference depending on the modeling and design needs. We provide an example of using SolTrace for modeling non-conventional receiver geometries. The goal is to transfer the irradiance profiles on the receiver surfaces calculated in an optical code to a computational fluid dynamics code such as ANSYS Fluent. This approach eliminates the need for using discrete ordinance or discrete radiation transfer models, which are computationally intensive, within the CFD code. The irradiance profiles on the receiver surfaces then allows for thermal and fluid analysis on the receiver.

Keywords: concentrating solar power, solar thermal, receiver, solar collector, solar concentrator

1. INTRODUCTION

Interest in and deployment of concentrating solar power (CSP) plants are on the rise in the US and worldwide.[1,2] CSP systems are complex having multiple subsystems that are optimally integrated for high system efficiency. The optical collectors/concentrators and receiver subsystems make up the front end of the CSP systems. It is important that the front end subsystems perform optimally; otherwise the efficiency of the rest of the systems for power production is reduced. Utility-scale deployment requires hundreds of mega-watts output from the plants.[2] Therefore, large CSP power plants require at least a million square meters of mirror reflective surface area, or hundreds of thousands of heliostats in a power tower plant as in the case of Brighsource's Ivanpah plant.[2] To ensure power production at high efficiencies from the plant, the performance of the optical collectors must be optimized. Optical errors such as alignment and surface slope errors have a large impact on the performance, which in most cases will not be completely understood during the design phase. The annual performance, an important metric of plant performance, may also not be well understood. This is where optical modeling and analysis tools become important and find their usefulness.[3-7]

Optical modeling tools help to understand the effects of the errors on the system performance and can quantify the daily and/or annual performance of the CSP system. In addition, some of the tools can be used to optimize and perform trade-offs on multiple design parameters based on cost and/or overall performance. Many optical modeling tools now exist on the market[7]. The commercial optical codes[8-10] are typically used to design and analyze general optical systems, and other codes are developed specifically for design and analysis of solar systems.[11-16] In this study we evaluated four optical modeling codes (suited for solar applications) and benchmarked them on a small heliostat field and flat plate receiver geometry. The four codes we evaluated are DELSOL[11], HELIOS[12], SolTrace[13-15], and Tonatiuh[15]. All these codes are available free of charge from their respective developers (see Table 1). There are multiple other codes that exist and are

* jeyello@sandia.gov; phone: 1-505-844-3029; fax: 1-505-844-3366; http://energy.sandia.gov/?page_id=2445

widely used for solar applications[7]. In the limited time that we had for our evaluation, we did not acquire and evaluate other codes such as MIRVAL, STRAL, or TieSOL.

DELSOL and HELIOS are considered first generation solar optical modeling codes developed by Sandia National Laboratories. HELIOS was initially developed in the late 1970's to evaluate the heliostat field at the National Solar Thermal Test Facility (NSTTF). It uses a cone optics approach (i.e. the error cone of the reflected "rays" is convolved with the sun shape) to calculate irradiance profiles on the receiver surface. The advantage of this approach is the computational speed. However, some approximations are carried out in the calculations, such as the normal probability distribution of the slope error on the mirror surfaces. Similarly, DELSOL uses Hermite polynomials to represent the irradiance distribution calculated through a convolution of the projection of the heliostat on the receiver, sunshape, and optical error distributions. The advantage here again is computational speed, but the flux profiles are approximated with truncated Hermite polynomials. DELSOL's introduction in the early 1980's was mainly due to a need for optimization capability and to quantify annual performance of the power tower designs. We used the latest version of the code, which is DELSOL3.

Ray-tracing methods pre-date other optical codes. However, commercial ray-tracing tools first found popularity in the aerospace community until the late 1980's for modeling complex optical systems. Ray-tracing is computationally intensive because calculations are performed at each ray-surface interaction. Many rays must be traced to construct meaningful irradiance distributions. Eventually codes more suitable for solar applications were developed, which most are made available for free, whereas the commercial codes can be expensive. Two of these solar optical codes are SolTrace by NREL and Tonatiuh by CENER. With modern computing advances, ray-tracing has become a viable option for modeling full CSP collector fields. Ray-tracing codes' potential lies in the flexibility and versatility in building more complex shapes and geometries. NREL lists this as the main reason for developing SolTrace.[14] The unique approach CENER is following is making Tonatiuh an open source code. This potentially could lead users to adapt the code towards their needs and preferences, making it more versatile over time; this remains to be seen in future releases. Table 1 summarizes the main features of the optical codes we evaluated.

This comparison study came about from our need to explore and model complex receiver geometries for power tower systems with the goal of reducing view factors and enhancing solar absorptance on the receivers.[17] Solar optical codes have been evaluated and compared in the past.[3-4] Typically, these evaluations were for a general need for modeling power tower systems, for example. Our evaluation was for a specific need to find a flexible tool to handle complex geometries. Consequently, we needed an optical modeling tool to help us design non-standard receivers and study their optical and thermal performance. Eventually the goal is to transfer the irradiance profiles calculated with optical codes to a computational fluid dynamics (CFD) code, and use the irradiance profiles as input boundary condition(s) for thermal and fluid analysis in the CFD code. In the following sections, we provide the results of our comparison of the optical codes. The comparison study helped us understand the strengths and deficiencies of the codes. In the Appendix we provide our initial modeling of two examples of non-standard receivers using SolTrace, and show an example of using both optical and CFD codes to perform optical and thermal analysis of complex receiver geometries.

2. APPROACH & METHOD

For our comparison study, we benchmarked the codes against a common solar collector field and a flat plate receiver. We modeled the NSTTF heliostat field and placed the receiver at the top of the 60 m central tower. The NSTTF heliostat field is a north-side field and contains 218 heliostats with each having 6.1 m × 6.1 m reflective area. For simplicity, we modeled the heliostats as monolithic flat surfaces (i.e. each heliostat is one big facet) instead of the 5×5 array of facets, which are each 1.22 m × 1.22 m in size. We assigned 1 mrad RMS slope error to the heliostats. The sunshape we used for all the codes is the Buie sunshape.[18] Tonatiuh uses this sunshape by default, and it was not apparent how the sunshape type can be changed easily. This limited the sunshape to the Buie type for this study. For the other three codes different sunshapes can be specified in a straight-forward manner by specifying the relative irradiance values versus the solar angle spread. Our sun position was at solar noon on Day 80 (spring equinox) in Albuquerque, NM at the NSTTF site (latitude = 34.96°). We set the incident irradiance to the standard terrestrial solar irradiance of 1000 W/m^2. The receiver type is a standard flat plate. The NSTTF tower is 60 m tall. We placed the receiver at the very top of the tower and moved 4 m forward towards the north – this placed it near the edge of the tower. The aimpoint for all the heliostats is geometrical center of the flat plate front surface. The receiver was sized to 11 m x 11 m (overall size) to collect the unfocused solar beams. Table 2 summarizes the baseline parameters that were used as input to the codes. To highlight the graphical capabilities of the ray-tracing codes, in Figure 1 we show the Tonatiuh and SolTrace plots of the heliostat field, tower, and receiver.

Table 1. Summary of the main features of the optical modeling codes we evaluated.

Optical Code	**DELSOL**	**HELIOS**	**SolTrace**	**Tonatiuh**
Method	Convolution: truncated Hermite polynomials	Convolution: cone optics	Ray-tracing	Ray-tracing
CSP system	Power tower systems	Power tower systems	Any CSP system and other general optical system	Any CSP system
Sampling at the receiver	Limited to 13x13 points.	11x11 points by default, but can be increased by stitching multiple grid arrays.	Up to 150x150 points max in steps of 5.	Sampling grid defined by user; 50x50 was used in this study.
Main features	Optimization and annual performance calculations.	NSTTF heliostat field is pre-defined, and includes atmospheric effects.	Many aperture and surface shapes, including measured surface data.	Open source code.
Developer	Sandia National Labs: energy.sandia.gov/ ?page_id=6530	Sandia National Labs: available by request	NREL: www.nrel.gov/csp /soltrace	CENER: code.google.com/p/ tonatiuh

Table 2. Baseline parameters used for the comparison study.

Sun Parameters	**Heliostat Field Parameters**	**Target Parameters**
• Buie sunshape • Day 80 at solar noon • Latitude = 34.96° • Insolation = 1000 W/m^2	• NSTTF heliostat field of 218 heliostats • Flat heliostats – modeled as one facet with 1 mrad RMS slope error • Heliostat size = 6.1 m x 6.1 m • Reflectance = 0.96	• Flat plate facing North (no tilt) • Size = 11 m x 11 m • Plate center position = (0,4,60) m, where (0,0,0) is the center of the tower base, z-axis points up and y-axis points North

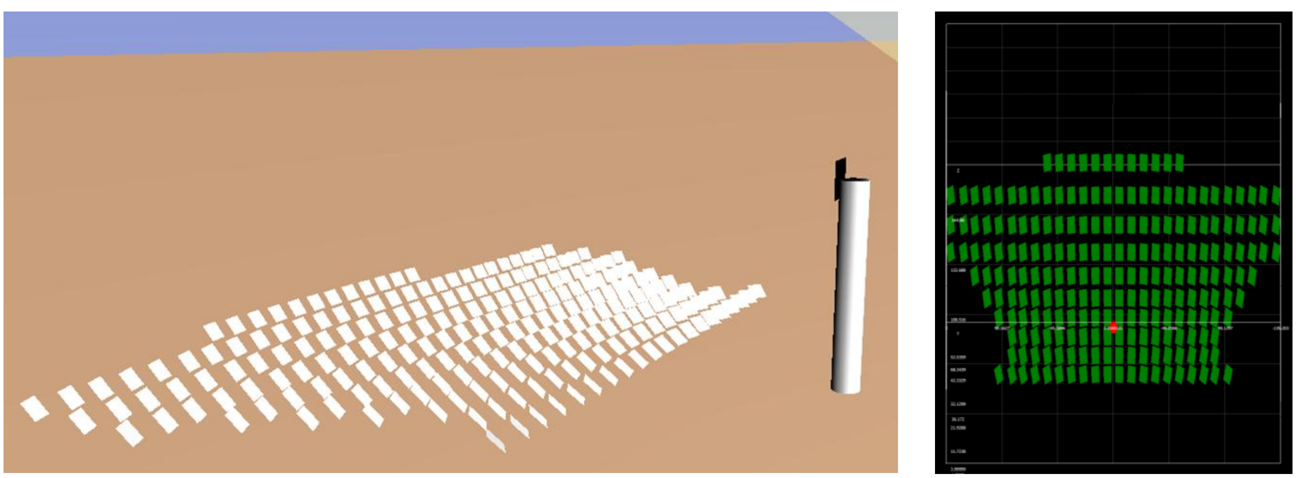

(a) (b)

Fig. 1. (a) Tonatiuh (view from the west side) and (b) SolTrace (top down view) graphical displays of the NSTTF field (218 heliostats), tower and flat plate receiver. Tonatiuh adds terrain and sky colors to the display which gives it some realism. SolTrace plots with a black background with separate colors for the "stages", and the axes auto-scales within a cube boundary.

3. RESULTS

3.1 Optical codes comparison

We benchmarked the four optical codes on the NSTTF heliostat field and a flat plate receiver located at the top of the tower. The resulting irradiance profiles from the codes are provided in Figure 2. The irradiance data were exported from each code, imported into Matlab and plotted over identical dimension and color scale. The colorbar scales were fixed to a range of 0 to 170 kW/m^2 on each plot. The grid size on the receiver for flux calculations is limited to 13×13 points for DELSOL; we used 11×11 here. The execution of our model in DELSOL was 1-2 seconds. The resulting flux profile is showing "hot" regions near the central portion causing a higher peak flux, and the edges appear to be more smoothed out compared to the flux profiles from the ray-tracing tools. HELIOS allows a sub-division of the facets. In this case, we represented the heliostat with one facet. We divided the facet into 21x21 sub-facets. With this number of sub-facets, HELIOS took about 10 seconds to execute. Increasing the number of sub-facets increases the processing time, but it provides higher accuracy in the irradiance profiles.

The SolTrace flux profile is showing a more pronounced rectangular profile. The ray intersections are binned into a grid array of 50×50 on the receiver. On a 32-bit machine, SolTrace appears to be limited to about 5 million traced rays. To trace 20 million rays, the model was run in batches. We ran the model five times with 5 million rays, changing the random number generator seed each time for the generation of the rays. Each batch run took about 2.5 minutes to complete on a 32-bit machine with an Intel i7 processor and eight cores. To trace the 20 million rays is then the equivalent of 10 minutes of run time. Twenty million rays were effectively traced to generate the flux profile shown in Figure 2. In our Tonatiuh set-up, 20 million rays were generated and traced all in one run. It ran in under 1 minute on a 64-bit machine with Intel i7 processor and eight cores. The output is a binary file that we read into Matlab to extract and plot the irradiance data. The ray intersections on the flat plate were binned into 50×50 grid points. Similar to SolTrace, the number of grid points on the receiver is user specified. The higher number of grid points provides a detailed profile of the flux, but the trade-off is the increase in the peak flux uncertainty. This can be seen in the flux profile in Figure 2 for Tonatiuh (i.e. various hot spots scattered over the flux profile). By reducing the number of grid points, the hot spots get smoothed out by averaging over the larger bins.

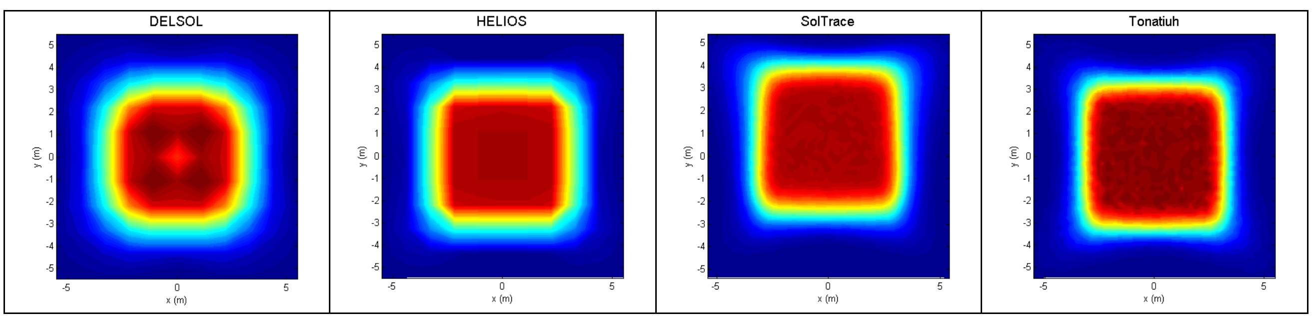

Fig. 2. Irradiance profiles from the four optical tools. The irradiance from the NSTTF field is incident a flat plat of size 11 m x 11 m. All four plots have the same x, y, (local coordinates of the receiver) and colorbar scales. Colorbar is scaled from 0 to 170 kW/m^2.

Table 3 summarizes the flux statistics (on the flat plate shown in Figure 2) from the four optical codes. The peak fluxes between the convolution methods varied substantially, but the average fluxes and the total power collected on the receiver are in closer agreement. DELSOL showed "hot" regions in the flux profile causing a large variation in the peak flux. The average fluxes for the ray-tracing codes agreed very well, but the peak fluxes varied more, although they agreed better than the convolution methods. Averaging of the SolTrace batch runs may have smoothed out the data, causing less uncertainty in the peak flux. To reduce the peak flux uncertainty, typically the number of gird bins at the receiver can be reduced. The total power collected for the ray-tracing codes also agree very well.

Table 3. Summary of the output irradiance and power values on a flat plate receiver. The heliostat facets are flat (i.e. non-focused).

Tool	Peak Flux (kW/m^2)	AVG Flux (kW/m^2)	Total Power (W)
DELSOL	178	53.4	7.17e+06
HELIOS	164	49.3	7.24e+06
SolTrace	168	62.4	7.34e+06
Tonatiuh	176	61.2	7.37e+06

4. DISCUSSION

The first generation codes (i.e. DELSOL and HELIOS) use style of creating input decks to execute the code. Input decks are highly formatted text files that contain information on the CSP system design, which the optical codes read in to perform the calculations. This is still a popular way to execute custom code, but can take some getting used to for inexperienced users. HELIOS is very sensitive to the text file formatting; it will not execute properly if a parameter field is exactly aligned to the specification. The debugging of the input deck then becomes tedious. DELSOL is more flexible on the formatting, but the variables must be named and ordered correctly. The computation speed of DELSOL and HELIOS is an advantage. Parameters can be changed rapidly and the code re-executed for quick analysis or optimization of the design. DELSOL has an optimization module that is useful. It also has a cost analysis module. The two modules combined provide optimizations on power tower system by balancing the cost and thermal performance of the system. A drawback of these codes is the lack of graphical tools, which modern ray-tracing codes typically have built in. The irradiance output must be exported to other tools such as Matlab or Excel to visualize and analyze the irradiance profiles.

The attractive feature of modern ray-tracing codes has been the graphical capabilities. Optical layouts can be plotted (as seen in Figure 1 from Tonatiuh and SolTrace) as well as the irradiance profiles within the code. Visually following the rays is also an efficient way of debugging the optical design. This is not possible with the first generation codes making debugging more difficult. With modern computing advances, millions of rays can be traced in minutes. The convolution methods, however, still have an advantage here where the execution time is seconds. Table 6 lists some of the strengths and deficiencies of the four optical codes.

Table 6. A short list of the strengths and disadvantages of the optical codes we evaluated.

Tool	DELSOL	HELIOS	SolTrace	Tonatiuh
Strengths	• Computation speed • Optimizes on heliostat layout, tower height, receiver size, storage size • Annual performance calculations	• Computation speed • NSTTF heliostat is pre-defined	• Graphical displays • More aperture and surface shapes available • Can import measured surface data • High resolution target sampling • Scripting	• Graphical displays • High resolution target sampling • Scripting • Open source code • Relatively fast ray tracing
Non-strengths	• Limited on surface shapes • Does not account for land slope • Limited target sampling • Flux is smoothed out due to approximations • Exportation of flux data needed	• Limited on surface shapes • Input deck very sensitive to formatting • Limited target sampling • Exportation of flux data needed	• 1,000,000+ rays needed to converge on results • Slow computation speed	• 1,000,000+ rays needed to converge on results

Finding a single tool to fit all the design and analysis needs may be difficult at present. Perhaps the choice of code to use can be based on a few criteria: 1) optimization of components and performance, 2) calculation of annual or instantaneous performance, or 3) geometry of components. For system optimizations, the convolution methods would be preferred for their rapid calculations of irradiance profiles. DELSOL has the advantage of using its optimization module. Ray-tracing tools, in theory, are capable of optimizations on designs; however, re-calculating irradiance profiles take considerable amount of time with these tools. The annual performance calculation engines are typically separate from the performance calculation modules. There are two ways to run the annual performance engine: as a one-time calculation, or as an optimization. For optimizations, the annual performance calculation engine is coupled with the thermal performance of the system and runs iteratively. It requires re-calculating the irradiance profiles with each iteration. In this sense, the convolution methods (i.e. DELSOL) have an advantage for annual performance optimizations. As a one-time annual performance calculation, both the convolution methods and ray-tracing tools are sufficient. Of the four tools we evaluated, DELSOL is the only tool capable of calculating annual performance on power tower systems.

Currently, the convolution methods do not have capability to model complex power tower receiver geometries; their pre-defined receivers are standard types such flat plate, external (cylindrical), and cavity receivers. However, it is not impossible to project the irradiance to any surface shape. By binning the angular content of the irradiance, the binned irradiance can be projected and intersected with any surface shape.[19] By using small bins, a sufficient detail of the flux can be mapped. This, however, will increase computation time as many bins would need to be generated and projected, and additions to the codes would have to be made to perform the binning and mapping calculations. In the case of ray-tracing, the single rays can easily be projected to virtually any surface and binned at the surface intersections. For this reason, the ray-tracing tools are more flexible for modeling complex shapes and are better suited for this purpose; an example of this is provided in the Appendix.

5. CONCLUSION & ON-GOING WORK

Concentrating solar power deployment is on the rise not only in the US, but worldwide. Optical modeling codes are needed to aid in understanding the error effects on the system performance as well as estimating the annual performance of the CSP system. As the CSP systems become more efficient, non-conventional receivers are being conceived and evaluated; they must be optically and thermally evaluated to improve their performance over conventional receivers.

We evaluated four optical codes and benchmarked them on the NSTTF heliostat field and flat plate receiver. This helped us understand the strengths and deficiencies of the codes. Two of the codes use convolution methods, and the other two use ray-tracing methods. Although still widely used, the older generation tools have become limited in some respects. The ray-tracing tools are proving to be more versatile in modeling complex shapes and geometries. The older tools are well suited for first-order designs and estimating annual performance, taking advantage of the computation speed. The ray-tracing tools at the moment are better suited for modeling advanced collector shapes and receiver geometries. We settled on using the ray-tracing tools to model our advanced receiver concepts and study the thermal performance. In terms of user-friendliness, SolTrace proved to be sufficient. The goal now is to use the irradiance profiles calculated with the optical code as input boundary conditions for thermal analysis in CFD codes. This approach shifts the optical modeling back to optical codes instead of in CFD codes using discrete ordinance or discrete radiative transfer models, which are computationally intensive especially for complex geometries over large spatial scales, and use the CFD code specifically for thermal and fluid analysis.

ACKNOWLEDGMENTS

Sandia National Laboratories is a multi-program laboratory managed and operated by Sandia Corporation, a wholly owned subsidiary of Lockheed Martin Corporation, for the U.S. Department of Energy's National Nuclear Security Administration under contract DE-AC04-94AL85000. The United States Government retains and the publisher, by accepting the article for publication, acknowledges that the United States Government retains a non-exclusive, paid-up, irrevocable, world-wide license to publish or reproduce the published form of this manuscript, or allow others to do so, for United States Government purposes.

REFERENCES

[1] Jacobson, M.Z. and Delucchi, M.A., "Providing All Global Energy," Energy Policy 39(3), 1154-1169 (2011).

[2] Mendelsohn, M., Lowder, T., and Canavan, B., "Utility-scale concentrating solar power and photovoltaics projects: a technology and market review," National Renewable Energy Laboratory, Golden, CO, NREL/TP-6A20-51137 (2012).

[3] Garcia, P., Ferriere, A., and Bezian, J-J, "Codes for solar flux calculation dedicated to central receiver system applications: A comparative review," Solar Energy 82(3), 189-197 (2013).

[4] Bode, S-J & Gauche, P., "Review of optical software for use in concentrating solar power systems," Proc. SASEC, 1-8 (2012).

[5] Lara Cerecedo, L.O., and et al., "Optical performance modeling of a solar tower heliostat field and estimation of receiver temperature," Proc. of IEEE Power, Electronics and Computing Conference, 1-6 (2013).

[6] Georgiou, M.D., Bonanos, A.M., and Georgiadis, J.G., "Optical evaluation of heliostat mirrors using caustics," J. Renewable Sustainable Energy 5(5), 053139 (2013).

[7] Ho, C.K., "Software and codes for analysis of concentrating solar power technologies," Sandia National Laboratories, Albuquerque, NM, SAND2008-8053 (2008).

[8] "FRED Software – Photon Engineering", Photon Engineering, 2014, http://www.photoengr.com/software.

[9] "Radiant Zemax", Radiant Zexmax, 1990, http://www.radiantzemax.com/zemax.

[10] "Breault Research Organization – ASAP Overview – Model Physical Optics, Imaging, and Illumination System," Breault, 2014, http://www.breault.com/software/asap-overview.php.

[11] Kistler, B.L., "A user's manual for DELSOL3: a computer code for calculating the optical performace and optical system design for solar thermal central receiver plants," Sandia National Laboratories, Albuquerque, NM, SAND86-8018 (1986).

[12] Vittitoe, C.N. and Biggs, F., "User's guide to HELIOS: a computer programs for modeling the optical behavior of reflecting solar concentrators," Sandia National Laboratories, Albuquerque, NM, SAND81-1562 (1981).

[13] "NREL: Concentrating Solar Power Research – SolTrace Home Page", NREL, 2012, http://www.nrel.gov/csp/soltrace.

[14] Wendelin, T. SolTRACE: A New Optical Modeling Tool for Concentrating Solar Optics. ASME 2003 International Solar Energy Conference, Solar Energy, Kohala Coast, Hawaii, USA, March 15–18, 2003.

[15] Wendelin, T., Dobos, A., & Lewandowski, A. (2013). SolTrace: a ray-tracing code for complex optical systems. Golden, CO: National Renewable Energy Laboratory, NREL/TP-5500-59163.

[16] "Tonatiuh – A Monte Carlo ray tracer for the optical simulation of solar concentrating systems", Google Code, http://www.google.com/p/tonatiuh.

[17] Ho, C.K., Christian, J.M., Ortega, J.D., Yellowhair, J., Mosquera, M.J., and Andraka, C.E., "Reduction of radiative heat losses for solar thermal receivers," Proc. SPIE, 1-10 (2104).

[18] Buie, D., Monger, A.G., and Dey, C.J., "Sunshape distribution for terrestrial solar simulations," Solar Energy 74(2), 113-122 (2003).

[19] Yellowhair, J. and Andraka, C.E., "Projection of flat-plane fluxmap images onto non-flat receiver surfaces," Proc. ASME ESFuelCell2011, 485-494 (2011).

[20] Mecit, A.M. and Miller, F., "A comparison between the Monte Carlo ray trace and the FLUENT discrete ordinates methods for treating solar input to a particle receiver," Proc. ASME ESFuelCell2014, 6412 (2014).

APPENDIX

A. MODELING OF COMPLEX RECEIVERS WITH SOLTRACE

Our current work on advanced receivers involves conceptualizing non-standard receiver shapes with the goal of reducing view factors and maximizing solar absorption. The strength of the ray-tracing tools for modeling complex shapes became apparent during our study. In this section, we show two examples of non-standard power tower receivers modeled and analyzed with SolTrace optical code. Figure 3a shows a star-shaped receiver modeled in SolidWorks; this geometry was incorporated into our SolTrace file. The Buie sunshape[18] with about 9.8 mrad angular spread was used as the source, and the NSTTF heliostat field as the collector field. Figure 3b shows reflected ray intersection points on the receiver surfaces to show the profile of the receiver shape. Since the NSTTF heliostat field is a north side field, only the north-facing half of the receiver was modeled in SolTrace. The flat surfaces that make up of the receiver are numbered 1-4. Figure 3c shows the irradiance projected onto the receiver flat surfaces. The receiver reflectivity was assumed to be 0.4, and multiple ray reflections off the walls were allowed. In this case all the heliostats are focused to slant range, and 1000 W/m^2 solar insolation was assumed. The single aimpoint for all the heliostats is at the center of mass of the receiver. SolTrace gives the option to show the net incident irradiance or net absorption on the receiver surfaces.

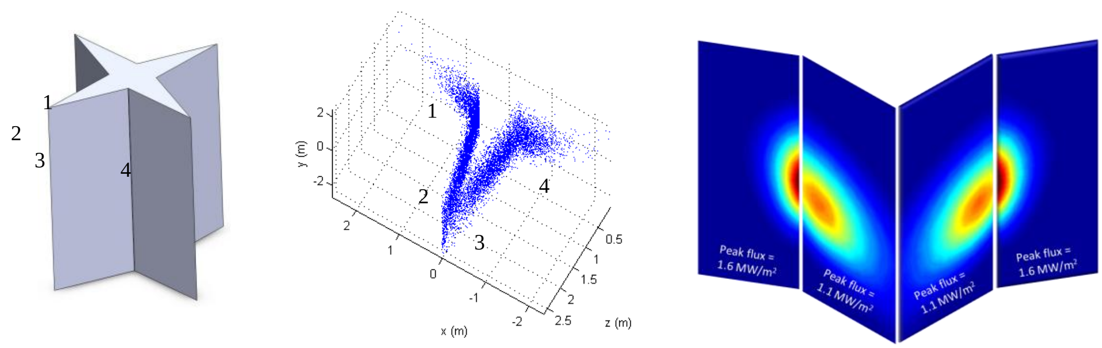

(a) (b) (c)

Fig. 3. (a) Solid model of the receiver, (b) SolTrace ray intersection points on the receiver, and (c) irradiance profiles on the flat surfaces of the receiver (colorbar on the plot is scaled from 0 to 1.5 MW/m^2).

Figure 4a shows an 8-finned receiver modeled in SolidWorks, which was incorporated into SolTrace. In SolTrace each fin is made up of two flat panels with a small gap in between to account for the fin thickness. The same input conditions as above were used in this model. Figure 4b shows reflected ray intersection points on the receiver surfaces to show the profile of the receiver shape. Again only the north-facing half of the receiver was modeled in SolTrace. The surfaces are numbered 1-8. Figure 4c shows the irradiance projected onto the receiver surfaces 1-4. Flux profiles on the other half (5-8) are nearly identical to the irradiance profiles shown, since the heliostat field is near symmetric and the sun is at solar noon. All the heliostats are focused to slant range, and 1000 W/m^2 solar insolation is assumed. The single aimpoint for all the heliostats is at the center of mass of the receiver.

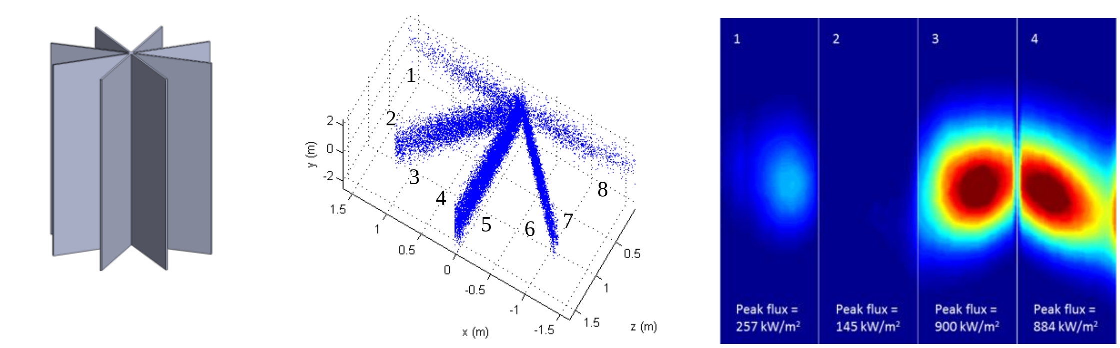

(a) (b) (c)

Fig. 4. (a) Solid model of the receiver, (b) SolTrace ray intersection points on the receiver, and (c) flux profiles on the flat surfaces (1-4) of the receiver (colorbar on each plot is scaled from 0 to 800 kW/m^2).

B. IRRADIANCE MAPPING FOR THERMAL ANALYSIS

The incident power absorbed by the receiver can be used as the boundary condition in computational fluid dynamics code for thermal analysis of the fluid flow in the receiver. Previous approaches have used discrete ordinance (DO) or discrete transfer radiation model (DRTM) methods to calculate the radiative transfer from the absorbed solar power through the receiver walls, which can be computationally intensive.[20] In addition, the accuracy of these methods depends largely on the number of rays traced for the discretization. For example, the number of phi (M) and theta (N) angle divisions in the DO model determines the number of equations to solve in ANSYS Fluent. In this case it would be MxNx8 (octants) equations of radiation per element that Fluent would need to solve.

We avoid this "ray tracing" model within the CFD codes. Our approach takes advantage of the strengths of the two analysis software: optical ray tracing and CFD codes. The receiver is first modeled in a CAD program. The receiver is reconstructed in the optical ray tracing code. The optical code is then used to calculate the irradiance absorbed by the receiver, which are binned. The number of bins over the receiver surface is set by the user. The irradiance comes from a solar collector field which reflects and concentrates the sunlight onto the receiver. A fraction of the incident irradiance is absorbed by the receiver. A MATLAB script was developed that reconstructs the geometry analyzed in SolTrace. The geometries are pre-generated using the stage file exported from SolTrace which provides the dimensions, solar direct normal incidence (DNI) value, and the number of bins used. The Matlab script also processes the 2-D mapped steady-state irradiance data, in local coordinates, obtained from SolTrace and map the values to the corresponding 3-D bins in global coordinates. The global coordinates (x, y, z), along with its corresponding heat flux value, are then written to a profile file which can be imported into Fluent. Within Fluent we evaluate the heat transfer to the fluid, convective and re-radiation losses. An example of this process is shown in Figure 5. It is very important to ensure the global coordinates of the geometry in Fluent match the coordinate system used in SolTrace to accurately map the irradiance profile on the surfaces. Since the profile will provide the boundary condition input for the Fluent model, the quality of the linear interpolation between bins will depend on the grid resolution specified in Fluent.

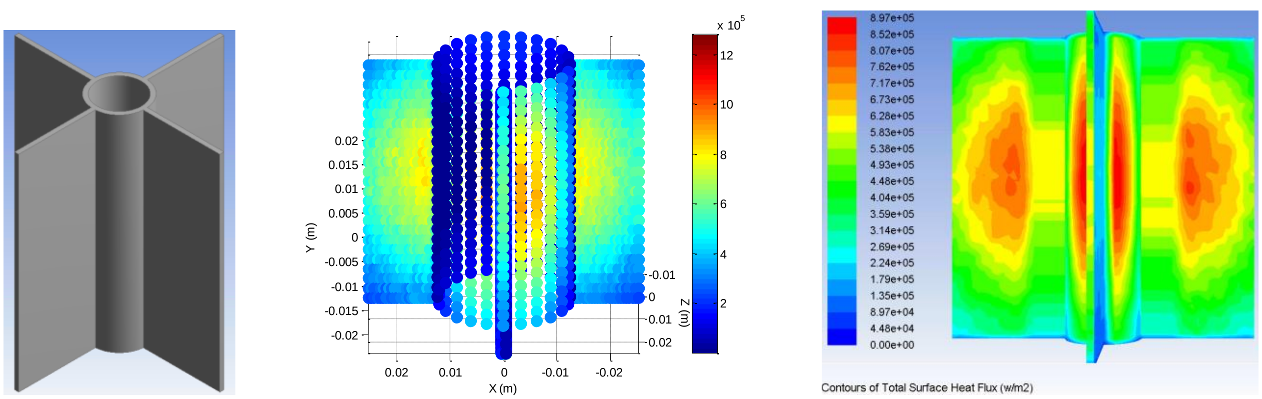

(a) (b) (c)

Fig. 5. (a) A solid model of a cylindrical receiver with fins. (b) Optical model of the receiver and irradiance mapped on the surfaces, and (c) the transfer of the irradiance profiles onto surfaces of the same receiver model in Fluent.